

9-20-2019

## The Fundamental Vibrational Frequencies and Spectroscopic Constants of the Dicyanoamine Anion, $\text{NCNCN}^-$ ( $\text{C}_2\text{N}_3^-$ ): Quantum Chemical Analysis for Astrophysical and Planetary Environments

David Dubois

*NASA Ames Research Center*

Ella Sciamma-O'Brien

*NASA Ames Research Center*

Ryan C. Fortenberry

*University of Mississippi*

Follow this and additional works at: [https://egrove.olemiss.edu/chem\\_facpubs](https://egrove.olemiss.edu/chem_facpubs)

---

### Recommended Citation

Dubois, D., Sciamma-O'Brien, E., & Fortenberry, R. C. (2019). The Fundamental Vibrational Frequencies and Spectroscopic Constants of the Dicyanoamine Anion,  $\text{NCNCN}^-$  ( $\text{C}_2\text{N}_3^-$ ): Quantum Chemical Analysis for Astrophysical and Planetary Environments. *The Astrophysical Journal*, 883(1), 109. <https://doi.org/10.3847/1538-4357/ab345e>

This Article is brought to you for free and open access by the Chemistry and Biochemistry at eGrove. It has been accepted for inclusion in Faculty and Student Publications by an authorized administrator of eGrove. For more information, please contact [egrove@olemiss.edu](mailto:egrove@olemiss.edu).



# The Fundamental Vibrational Frequencies and Spectroscopic Constants of the Dicyanoamine Anion, NCNCN<sup>−</sup> (C<sub>2</sub>N<sub>3</sub><sup>−</sup>): Quantum Chemical Analysis for Astrophysical and Planetary Environments

David Dubois<sup>1,2</sup> , Ella Sciamma-O’Brien<sup>1</sup>, and Ryan C. Fortenberry<sup>3</sup>

<sup>1</sup> NASA Ames Research Center, Space Science & Astrobiology Division, Astrophysics Branch, Moffett Field, CA 94035, USA

<sup>2</sup> Bay Area Environmental Research Institute, Moffett Field, CA 94035, USA

<sup>3</sup> Department of Chemistry & Biochemistry, University of Mississippi, University, MS 38677-1848, USA; [r410@olemiss.edu](mailto:r410@olemiss.edu)

Received 2019 June 12; revised 2019 July 10; accepted 2019 July 22; published 2019 September 25

## Abstract

Detecting anions in space has relied on a strong collaboration between theoretical and laboratory analyses to measure rotational spectra and spectroscopic constants to high accuracy. The advent of improved quantum chemical tools operating at higher accuracy and reduced computational cost is a crucial solution for the fundamental characterization of astrophysically relevant anions and their detection in the interstellar medium (ISM) and planetary atmospheres. In this context, we have turned toward the quantum chemical analysis of the pentatomic dicyanoamine anion NCNCN<sup>−</sup> (C<sub>2</sub>N<sub>3</sub><sup>−</sup>), a structurally bent and polar compound. We have performed high-level coupled cluster theory quartic force field computations of C<sub>2</sub>N<sub>3</sub><sup>−</sup> satisfying both computational cost and accuracy conditions. We provide for the first time accurate spectroscopic constants and vibrational frequencies for this ion. In addition to exhibiting various Fermi resonances, C<sub>2</sub>N<sub>3</sub><sup>−</sup> displays a bright  $\nu_2$  (2130.9 cm<sup>−1</sup>) and a less intense  $\nu_1$  (2190.7 cm<sup>−1</sup>) fundamental vibrational frequency, making for strong markers for future infrared observations <5  $\mu$ m. We have also determined near-IR overtone and combination bands of the bright fundamentals for which the  $2\nu_2$  at 4312.1 cm<sup>−1</sup> (2.319  $\mu$ m) is the best candidate. C<sub>2</sub>N<sub>3</sub><sup>−</sup> could potentially exist and be detected in nitrogen-rich environments of the ISM such as IRC +10216 and other carbon-rich circumstellar envelopes, or in the atmosphere of Saturn’s moon Titan, where advanced N-based reactions may lead to its formation.

*Unified Astronomy Thesaurus concepts:* Interstellar molecules (849); Molecular gas (1073); Interstellar medium (847); Planetary atmospheres (1244)

## 1. Introduction

The chemical reservoir of negative ions in the universe encompasses a broad range of astrophysical and astrochemical environments: from cold interstellar clouds, circumstellar envelopes (CSE), and carbon-rich Asymptotic Giant Branch stars, to cometary comae and planetary atmospheres. The combined theoretical and experimental prospect for their spectroscopic characterization has resulted in unprecedented observations of key cosmic anions in the aforementioned environments (see the review by Millar et al. 2017 and references therein).

Since the first anion observations in dense molecular clouds and CSE in 2006 (McCarthy et al. 2006), their detection has remained difficult. The well-studied IRC +10216 CSE (e.g., Remijan et al. 2007) has nonetheless revealed the presence of C<sub>n</sub>H<sup>−</sup> carbon-chain as well as C<sub>n−1</sub>N<sup>−</sup> cyano molecular anions (e.g., Thaddeus et al. 2008) with  $n = 2$ –6. Among these, C<sub>8</sub>H<sup>−</sup> (Brünken et al. 2007) represents the largest carbon-chain anion detected in the interstellar medium. Molecular anions containing multiple nitrogen atoms are still elusive as their experimental and theoretical spectroscopic constants are no yet available to guide observations.

The direct and indirect molecular study of C<sub>2</sub>N<sub>3</sub><sup>−</sup> can be traced back to work carried out over the past two centuries, with a specific emphasis on the understanding of peptide and polypeptide synthesis. Historically, interest was drawn upon cyanamide CH<sub>2</sub>N<sub>2</sub> as early as 1858, when cyanamide was shown to readily dimerize into dicyanamide C<sub>2</sub>N<sub>3</sub>H (Beilstein & Geuther 1858). It was not until 1922 that a first synthesis scheme for this molecule and a series of other H<sub>x</sub>C<sub>y</sub>N<sub>z</sub> compounds involving de-ammonated reactions were proposed, for which a C<sub>2</sub>N<sub>3</sub> nucleus was identified

(Franklin 1922). These derivatives were further investigated by Steinman et al. (1966) and Steinman & Cole (1967) in the study of dicyanamide as an intermediate in the synthesis of polypeptides such as diglycine in the primitive Earth environment. Their scheme also included the dicyanoamine anion NCNCN<sup>−</sup>. Henceforth, C<sub>2</sub>N<sub>3</sub>H and C<sub>2</sub>N<sub>3</sub><sup>−</sup> were determined to be important precursors in the prebiotic chemical evolution leading to the formation of peptides. Schimpl et al. (1965) also investigated the formation of cyanamide under primitive Earth conditions. In addition, reactive and thermodynamic properties of NCNCN<sup>−</sup> in ionic liquids were investigated by Dahl et al. (2005), Jagoda-Cwiklik et al. (2007), and Nichols et al. (2016).

Recently, observations from the *Cassini* mission unveiled the presence of unidentified large anions with masses up to 13,800  $u/q$  at high altitude (>950 km) in the atmosphere of Titan, Saturn’s largest moon (Coates et al. 2007). Recent work has helped characterize observed mass peaks and growth patterns in relation to ion N-based reactions (Lavvas et al. 2013; Desai et al. 2017; Dubois et al. 2019). Furthermore, C<sub>2</sub>N<sub>3</sub><sup>−</sup> was reportedly identified as a potential precursor seed fragment in the polymeric growth of laboratory-produced atmospheric aerosols, analogs of Titan’s atmospheric haze (Carrasco et al. 2009; Somogyi et al. 2012).

While even available for purchase from many chemical companies as a solid salt of sodium dicyanoamide, the gas phase vibrational and rotational spectra of this molecule have yet to be conclusively provided. Such spectroscopic data would be required for any future observations of this molecule in planetary atmospheres, CSEs, or other astrophysical environments. As such, the work presented here relies upon proven

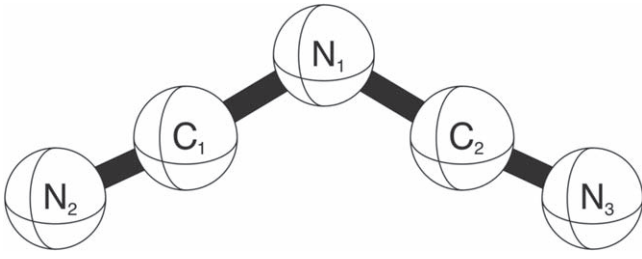


Figure 1. Equilibrium structure of  $\text{NCNCN}^-$ .

quantum chemical tools for the predictions of these values. The established CcCR approach utilizes a quartic force field (QFF, fourth-order Taylor series expansion of the internuclear Hamiltonian) comprised of energy points defined from quantum chemical complete basis set extrapolation (“C”), inclusion of core-electron correlation (“cC”), and considerations for scalar relativity (“R”) (Huang & Lee 2008, 2009; Fortenberry et al. 2011; Huang et al. 2011). This method has produced vibrational frequencies to within  $1.0\text{ cm}^{-1}$  and rotational constants within 10 MHz of gas phase experiment in many cases (Huang & Lee 2008, 2009; Huang et al. 2011, 2013; Fortenberry et al. 2012, 2014a, 2015a; Zhao et al. 2014; Kitchens & Fortenberry 2016; Bizzocchi et al. 2017; Fortenberry 2017). Recently, the use of explicitly correlated electron wavefunctions has promised an increase in quantum chemical accuracy at significantly reduced computational cost. Contemporary work has shown that the coupled cluster singles, doubles, and perturbative triples [CCSD(T)] method (Raghavachari et al. 1989) within the F12 explicitly correlated formalism (Adler et al. 2007; Knizia et al. 2009; Kong et al. 2011) is typically within  $6.0\text{ cm}^{-1}$  or better of the expected CcCR results but with orders of magnitude reduction in computational time (Agbaglo & Fortenberry 2019; Agbaglo et al. 2019). As such, both highly accurate approaches are employed here to produce the necessary vibrational and rotational spectroscopic data for  $\text{NCNCN}^-$  in order to aid in its potential classification in the atmosphere of Titan, IRC +10216, or other celestial objects.

## 2. Computational Details

The two different approaches used in this study are detailed hereafter. The QFF procedure begins with a geometry optimization and construction of the reference geometry. The CcCR geometry is defined from a CCSD(T)/aug-cc-pV5Z (Dunning 1989; Kendall et al. 1992) minimum further corrected for core correlation from optimizations with the Martin–Taylor (MT) core correlating basis set (Martin & Taylor 1994) both including and excluding the core electrons. The CCSD(T)-F12/cc-pVTZ-F12 (denoted as F12-TZ from here on) QFF, on the other hand, begins simply with an optimized minimum at this level of theory with no further corrections. Regardless of the method, the QFF is defined from 1585 points based on displacements of the reference geometry using the below  $S_i$  symmetry-internal coordinates defined by Equations (1)–(9) and an efficient lazy-Cartesian algorithm to construct the displacements (Thackston & Fortenberry 2018). The bond lengths are displaced by  $0.005\text{ \AA}$  and the angles as well as the in-plane (LINX) and out-of-plane (LINY) near-linear bends are displaced by  $0.005$  radians. The atom numbering and symmetry-internal coordinates,  $a_i$  and  $b_i$ , in this

$\text{C}_{2v}$  molecule are done according to Figure 1

$$S_1(a_1) = C_1 - C_2 \quad (1)$$

$$S_2(a_1) = \frac{1}{\sqrt{2}}[(N_1 - C_1) + (N_1 - C_2)] \quad (2)$$

$$S_3(a_1) = \frac{1}{\sqrt{2}}[(C_1 - N_2) + (C_2 - N_3)] \quad (3)$$

$$S_4(a_1) = \frac{1}{\sqrt{2}}[\text{LINX}(N_2 - C_1 - N_1 - C_2) + \text{LINX}(N_3 - C_2 - N_1 - C_1)] \quad (4)$$

$$S_5(b_2) = \frac{1}{\sqrt{2}}[(N_1 - C_1) - (N_1 - C_2)] \quad (5)$$

$$S_6(b_2) = \frac{1}{\sqrt{2}}[(C_1 - N_2) - (C_2 - N_3)] \quad (6)$$

$$S_7(b_2) = \frac{1}{\sqrt{2}}[\text{LINX}(N_2 - C_1 - N_1 - C_2) - \text{LINX}(N_3 - C_2 - N_1 - C_1)] \quad (7)$$

$$S_8(b_1) = \frac{1}{\sqrt{2}}[\text{LINY}(N_2 - C_1 - N_1 - C_2) - \text{LINY}(N_3 - C_2 - N_1 - C_1)] \quad (8)$$

$$S_9(a_2) = \frac{1}{\sqrt{2}}[\text{LINY}(N_2 - C_1 - N_1 - C_2) + \text{LINY}(N_3 - C_2 - N_1 - C_1)]. \quad (9)$$

Similar internal coordinates have been used in cyclopropenyliene and its silylated cousin  $c\text{-SiC}_2\text{H}_2$  (Fortenberry et al. 2018a, 2018b). The LINX and LINY coordinates have been defined previously by Fortenberry et al. (2012).

The CcCR QFF requires seven energy computations at each point. The CCSD(T)/aug-cc-pVTZ, -pVQZ, and -pV5Z energies are extrapolated to the complete basis set (CBS) limit via a three-point formula (Martin & Lee 1996). The differences in the CCSD(T)/MT energies are then added to this CBS energy, as are differences in the CCSD(T)/cc-pVTZ-DK energies (Douglas & Kroll 1974; de Jong et al. 2001) with and without relativity included. This molecule represents the most basis functions ever utilized for a full CcCR QFF computation. Again, the F12-TZ QFF only requires the CCSD(T)-F12/cc-pVTZ-F12 energies to be computed reducing the computation time of the QFF from roughly two months in the CcCR approach to two days with F12-TZ. The CcCR center-of-mass dipole moment is computed at the equilibrium geometry defined below with the CCSD(T)/aug-cc-pV5Z level of theory. The F12-TZ dipole moment is computed at its optimized geometry. All of the electronic structure computations described thus far employ the MOLPRO 2015.1 electronic structure program (Werner et al. 2012, 2015). The double-harmonic intensities of the vibrational frequencies are computed with MP2/6-31+G(d) in the Gaussian09 program (Møller & Plesset 1934; Hehre et al. 1972; Frisch et al. 2009) and are known to closely mirror experimental and higher-order quantum chemical values (Fortenberry et al. 2014b; Yu et al. 2015; Finney et al. 2016).

Once the points are generated and the energies compiled, the total energies are zeroed to the minimum energy, producing relative energies, which reduces the possible numerical noise in the computation. Then, a least squares fit procedure with a sum of squared residuals on the order of  $10^{-17}\text{ au}^2$  for CcCR and

$10^{-18} \text{ au}^2$  for F12-TZ is refit to the new minimum producing the necessary force constants for the actual Taylor series definition of the potential. Transformation of the force constants into Cartesian derivatives via the Intder program (Allen 2005) allows for more flexible usage of the potential within the Spectro program (Gaw et al. 1991). Spectro utilizes rotational and vibrational perturbation theory at second order (VPT2; Mills 1972; Watson 1977; Papoušek & Aliev 1982) to produce the observable spectroscopic values. NCNCN<sup>-</sup> exhibits a  $2\nu_6 = 2\nu_7 = 2\nu_8 = \nu_4$  Fermi resonance polyad, a  $\nu_4 + \nu_3 = \nu_2$  type-2 Fermi resonance, and a  $\nu_8 + \nu_4 = \nu_8 + \nu_5 = \nu_3$  Fermi resonance polyad. Additionally, four Coriolis resonances are also treated in this system:  $\nu_6/\nu_5$  B-type,  $\nu_7/\nu_5$  A-type,  $\nu_8/\nu_6$  A-type, and  $\nu_8/\nu_7$  B-type. The inclusion of these resonances has been shown to further improve the accuracy of QFF VPT2-type approaches markedly (Maltseva et al. 2015).

### 3. Results

#### 3.1. Structure and Rotational Spectroscopic Constants

NCNCN<sup>-</sup> is a near-prolate molecule of likely high detectability. -CN groups have been some of the most observed functional groups to date in interstellar molecules (McGuire 2018), and the anion of interest here has two. According to Table 1, the CcCR C $\equiv$ N bond lengths of 1.17264 Å are nearly exactly the value expected for such bonding, like in the 1.172 Å bond length in the cyano radical (Huber et al. 2018), and they are very nearly the same for F12-TZ. Additionally, the  $F_{33}$  force constant in Table 2 is rather large at 16.514 mdyne Å<sup>-2</sup> indicating very strong bonding typical of a cyano group. In comparison, Fortenberry et al. (2013) had calculated an  $F_{33}$  force constant of 15.589 mdyne Å<sup>-2</sup> for the cyanomethyl anion CH<sub>2</sub>CN<sup>-</sup>. The N<sub>1</sub>-C<sub>1/2</sub> bonding is also strong at 7.036 mdyne Å<sup>-2</sup>, but this is closer to the values expected of a single bond as the Lewis structure of this molecule would indicate. The triple bond also produces a near-linearity in the  $\angle(\text{N}_1-\text{C}_{1/2}-\text{N}_{2/3})$  bond angles which are 174.04° in line with previous work. The rest of the F12-TZ force constants necessary for the Spectro computations are in Table 2.

The structure of this molecule from such near-linearities lends itself to being near-prolate as the rotational constants in Table 1 indicate. The  $B$  and  $C$  rotational constants are a factor of more than 13 less than the  $A$  constant indicating that the K-branching would typically be small and potentially non-existent at lower resolutions. However, the 1.03  $D$  dipole moment is aligned along the  $C$  rotational axis and therefore the analysis of any future observed rotational spectrum of this molecule will require all three constants to fit its Hamiltonian. This molecule has the potential to be observable with ground-based radio telescopes. Even though the F12-TZ rotational constants are known to not be as good as the CcCR values unlike the vibrational frequencies (Agbaglo & Fortenberry 2019) which are discussed below, the  $B$  and  $C$  constants vary by around only 10 MHz between the QFFs. The quartic and sextic distortion constants ( $D$  and  $H$ ) as well as the vibrationally excited rotational constants (numbered from Table 3) are also given in Table 1. These distortions are relatively small due to the rigidity of the molecule. The vibrationally excited  $B$  and  $C$  constants do not vary greatly with vibrational excitation, but the  $A$  constants oscillate by as much as 3000 MHz from mode to mode.

**Table 1**  
The CcCR and F12/TZ Equilibrium and Vibrationally Averaged ( $R_v$ )  
Structural and Rotational Spectroscopic Constants

|  | Units | CcCR    | F12-TZ  |
|--|-------|---------|---------|
| $r_e(\text{N}_1-\text{C}_{1/2})$                     | Å     | 1.31467 | 1.31834 |
| $r_e(\text{C}_{1/2}-\text{N}_{2/3})$                 | Å     | 1.17199 | 1.17504 |
| $\angle_e(\text{C}_1-\text{N}_1-\text{C}_2)$         | °     | 118.82  | 118.50  |
| $\angle_e(\text{N}_1-\text{C}_{1/2}-\text{N}_{2/3})$ | °     | 174.12  | 174.01  |
| $A_e$  | MHz   | 39786.3 | 39290.3 |
| $B_e$  | MHz   | 3047.3  | 3038.1  |
| $C_e$  | MHz   | 2830.5  | 2820.0  |
| $D_J$  | kHz   | 1.290   | 1.282   |
| $D_{JK}$   | MHz   | -0.152  | -0.148  |
| $D_K$  | MHz   | 6.009   | 5.778   |
| $d_1$  | kHz   | -0.294  | -0.294  |
| $d_2$  | kHz   | -0.005  | -0.005  |
| $H_J$  | mHz   | 3.753   | 3.738   |
| $H_{JK}$   | Hz    | -0.083  | -0.089  |
| $H_{KJ}$   | Hz    | -60.234 | -56.845 |
| $H_K$  | kHz   | 2.952   | 2.754   |
| $h_1$  | mHz   | 1.415   | 1.412   |
| $h_2$  | mHz   | 0.061   | 0.062   |
| $h_3$  | mHz   | 0.023   | 0.023   |
| $\mu$  | D     | 1.03    | 1.02    |
| $r_0(\text{N}_1-\text{C}_{1/2})$                     | Å     | 1.31868 | 1.32234 |
| $r_0(\text{C}_{1/2}-\text{N}_{2/3})$                 | Å     | 1.17264 | 1.17560 |
| $\angle_0(\text{C}_1-\text{N}_1-\text{C}_2)$         | °     | 118.78  | 118.46  |
| $\angle_0(\text{N}_1-\text{C}_{1/2}-\text{N}_{2/3})$ | °     | 174.04  | 173.94  |
| $A_0$  | MHz   | 40289.7 | 39776.3 |
| $B_0$  | MHz   | 3037.4  | 3028.5  |
| $C_0$  | MHz   | 2819.0  | 2808.8  |
| $A_1$  | MHz   | 40228.9 | 39713.8 |
| $B_1$  | MHz   | 3025.6  | 3016.8  |
| $C_1$  | MHz   | 2808.6  | 2798.4  |
| $A_2$  | MHz   | 39938.8 | 39435.6 |
| $B_2$  | MHz   | 3029.7  | 3020.7  |
| $C_2$  | MHz   | 2810.6  | 2800.4  |
| $A_3$  | MHz   | 38738.7 | 38268.8 |
| $B_3$  | MHz   | 3052.5  | 3043.3  |
| $C_3$  | MHz   | 2824.6  | 2814.3  |
| $A_4$  | MHz   | 41207.2 | 40660.4 |
| $B_4$  | MHz   | 3017.2  | 3008.6  |
| $C_4$  | MHz   | 2804.2  | 2794.2  |
| $A_5$  | MHz   | 41093.4 | 40558.2 |
| $B_5$  | MHz   | 3026.5  | 3017.7  |
| $C_5$  | MHz   | 2812.9  | 2802.8  |
| $A_6$  | MHz   | 40102.4 | 39604.7 |
| $B_6$  | MHz   | 3043.0  | 3034.2  |
| $C_6$  | MHz   | 2824.0  | 2814.0  |
| $A_7$  | MHz   | 40769.0 | 40242.9 |
| $B_7$  | MHz   | 3029.4  | 3021.0  |
| $C_7$  | MHz   | 2816.4  | 2806.6  |
| $A_8$  | MHz   | 40112.1 | 39606.5 |
| $B_8$  | MHz   | 3045.4  | 3036.4  |
| $C_8$  | MHz   | 2823.7  | 2813.5  |
| $A_9$  | MHz   | 41424.5 | 40867.9 |
| $B_9$  | MHz   | 3047.4  | 3038.7  |
| $C_9$  | MHz   | 2823.2  | 2813.0  |

#### 3.2. Fundamental Vibrational Frequencies

NCNCN<sup>-</sup> has an exceptionally bright  $\nu_2$  fundamental vibrational frequency at 2130.9 cm<sup>-1</sup> or 4.693 μm. The intensity is predicted to be on the order of that expected for exotic species like proton-bound complexes (Fortenberry et al. 2015b; Yu et al. 2015; McDonald et al. 2016; Stephan & Fortenberry 2017) and

**Table 2**  
The F12-TZ Force Constants (in mdyne/Å<sup>2</sup> rad<sup>m</sup>) with the Indices Corresponding to the Coordinate Numbers Given in the Text

|           |           |            |          |            |        |            |        |            |       |
|-----------|-----------|------------|----------|------------|--------|------------|--------|------------|-------|
| $F_{11}$  | 1.569243  | $F_{661}$  | 0.0091   | $F_{4311}$ | 0.48   | $F_{6643}$ | -0.11  | $F_{8821}$ | -0.17 |
| $F_{21}$  | -0.401374 | $F_{662}$  | -0.2649  | $F_{4321}$ | -0.51  | $F_{6644}$ | -0.01  | $F_{8822}$ | 0.28  |
| $F_{22}$  | 7.035627  | $F_{663}$  | -77.8702 | $F_{4322}$ | 0.90   | $F_{6655}$ | 2.45   | $F_{8831}$ | -0.15 |
| $F_{31}$  | -0.141918 | $F_{664}$  | -0.1133  | $F_{4331}$ | 0.21   | $F_{6665}$ | -1.72  | $F_{8832}$ | 1.05  |
| $F_{32}$  | 0.689322  | $F_{751}$  | 0.2937   | $F_{4332}$ | -0.25  | $F_{6666}$ | 300.54 | $F_{8833}$ | 0.18  |
| $F_{33}$  | 16.514247 | $F_{752}$  | -0.4648  | $F_{4333}$ | -0.03  | $F_{7511}$ | 0.09   | $F_{8841}$ | -0.02 |
| $F_{41}$  | 0.110356  | $F_{753}$  | 0.0150   | $F_{4411}$ | 0.65   | $F_{7521}$ | -0.72  | $F_{8842}$ | 0.14  |
| $F_{42}$  | 0.089479  | $F_{754}$  | -0.6003  | $F_{4421}$ | -0.70  | $F_{7522}$ | 1.66   | $F_{8843}$ | 0.08  |
| $F_{43}$  | 0.065200  | $F_{761}$  | -0.0776  | $F_{4422}$ | 1.04   | $F_{7531}$ | 0.12   | $F_{8844}$ | 0.49  |
| $F_{44}$  | 0.561455  | $F_{762}$  | -0.0910  | $F_{4431}$ | -0.02  | $F_{7532}$ | -0.11  | $F_{8855}$ | 0.37  |
| $F_{55}$  | 8.015981  | $F_{763}$  | -0.0639  | $F_{4432}$ | 0.73   | $F_{7533}$ | 0.11   | $F_{8865}$ | 0.64  |
| $F_{65}$  | 0.954895  | $F_{764}$  | -0.7086  | $F_{4433}$ | 0.12   | $F_{7541}$ | -0.11  | $F_{8866}$ | 0.10  |
| $F_{66}$  | 16.160572 | $F_{771}$  | 0.0700   | $F_{4441}$ | 0.12   | $F_{7542}$ | 0.98   | $F_{8875}$ | -0.10 |
| $F_{75}$  | 0.028367  | $F_{772}$  | -0.7099  | $F_{4442}$ | 0.16   | $F_{7543}$ | 0.56   | $F_{8876}$ | 0.06  |
| $F_{76}$  | 0.059044  | $F_{773}$  | -0.8253  | $F_{4443}$ | 0.17   | $F_{7544}$ | 0.10   | $F_{8877}$ | 0.54  |
| $F_{77}$  | 0.559994  | $F_{774}$  | -0.2081  | $F_{4444}$ | 1.50   | $F_{7555}$ | -0.24  | $F_{8888}$ | 1.66  |
| $F_{88}$  | 0.584796  | $F_{881}$  | -0.0435  | $F_{5511}$ | 2.40   | $F_{7611}$ | -0.09  | $F_{9851}$ | 0.08  |
| $F_{99}$  | 0.636805  | $F_{882}$  | -0.5506  | $F_{5521}$ | 0.15   | $F_{7621}$ | -0.07  | $F_{9852}$ | 0.79  |
| $F_{111}$ | 1.0720    | $F_{883}$  | -0.7621  | $F_{5522}$ | 131.56 | $F_{7622}$ | 0.41   | $F_{9853}$ | 0.56  |
| $F_{211}$ | -1.7283   | $F_{884}$  | -0.0571  | $F_{5531}$ | -0.79  | $F_{7631}$ | -0.01  | $F_{9854}$ | 0.13  |
| $F_{221}$ | -0.8397   | $F_{985}$  | -0.8259  | $F_{5532}$ | 3.72   | $F_{7632}$ | -0.01  | $F_{9861}$ | -0.18 |
| $F_{222}$ | -31.2465  | $F_{986}$  | -0.5932  | $F_{5533}$ | 0.51   | $F_{7633}$ | -0.10  | $F_{9862}$ | 0.61  |
| $F_{311}$ | -0.8862   | $F_{987}$  | -0.0609  | $F_{5541}$ | 0.17   | $F_{7641}$ | 0.12   | $F_{9863}$ | -0.02 |
| $F_{321}$ | 1.3618    | $F_{991}$  | -0.0345  | $F_{5542}$ | -0.37  | $F_{7642}$ | 0.54   | $F_{9864}$ | 0.07  |
| $F_{322}$ | -3.0329   | $F_{992}$  | -0.5765  | $F_{5543}$ | 0.09   | $F_{7643}$ | -0.04  | $F_{9871}$ | -0.02 |
| $F_{331}$ | -0.1273   | $F_{993}$  | -0.8648  | $F_{5544}$ | -0.04  | $F_{7644}$ | 0.09   | $F_{9872}$ | 0.13  |
| $F_{332}$ | -0.7153   | $F_{994}$  | -0.1138  | $F_{5555}$ | 117.81 | $F_{7655}$ | -0.15  | $F_{9873}$ | 0.05  |
| $F_{333}$ | -78.3673  | $F_{1111}$ | 5.27     | $F_{6511}$ | 0.93   | $F_{7665}$ | -0.01  | $F_{9874}$ | 0.47  |
| $F_{411}$ | -0.3095   | $F_{2111}$ | -2.40    | $F_{6521}$ | -0.84  | $F_{7666}$ | -0.18  | $F_{9911}$ | -0.02 |
| $F_{421}$ | 0.4662    | $F_{2211}$ | -1.74    | $F_{6522}$ | 3.14   | $F_{7711}$ | 0.74   | $F_{9921}$ | 0.00  |
| $F_{422}$ | -1.0531   | $F_{2221}$ | 10.99    | $F_{6531}$ | -0.42  | $F_{7721}$ | -0.97  | $F_{9922}$ | -0.10 |
| $F_{431}$ | -0.1847   | $F_{2222}$ | 102.54   | $F_{6532}$ | 2.88   | $F_{7722}$ | 1.49   | $F_{9931}$ | -0.22 |
| $F_{432}$ | -0.0670   | $F_{3111}$ | -0.51    | $F_{6533}$ | -1.42  | $F_{7731}$ | -0.21  | $F_{9932}$ | 1.19  |
| $F_{433}$ | -0.0812   | $F_{3211}$ | 2.97     | $F_{6541}$ | -0.13  | $F_{7732}$ | 1.16   | $F_{9933}$ | 0.13  |
| $F_{441}$ | -0.0244   | $F_{3221}$ | -7.56    | $F_{6542}$ | 0.07   | $F_{7733}$ | 0.10   | $F_{9941}$ | 0.07  |
| $F_{442}$ | -0.5255   | $F_{3222}$ | 15.94    | $F_{6543}$ | -0.09  | $F_{7741}$ | -0.07  | $F_{9942}$ | 0.11  |
| $F_{443}$ | -0.8250   | $F_{3311}$ | -0.73    | $F_{6544}$ | 0.74   | $F_{7742}$ | 0.40   | $F_{9943}$ | 0.06  |
| $F_{444}$ | -0.1967   | $F_{3321}$ | 0.44     | $F_{6555}$ | 3.21   | $F_{7743}$ | 0.20   | $F_{9944}$ | 0.54  |
| $F_{551}$ | -1.0580   | $F_{3322}$ | 1.23     | $F_{6611}$ | 0.05   | $F_{7744}$ | 1.57   | $F_{9955}$ | 0.42  |
| $F_{552}$ | -35.9427  | $F_{3331}$ | 0.11     | $F_{6621}$ | -1.03  | $F_{7755}$ | 0.16   | $F_{9965}$ | 0.82  |
| $F_{553}$ | -2.4013   | $F_{3332}$ | 0.19     | $F_{6622}$ | 3.02   | $F_{7765}$ | 0.69   | $F_{9966}$ | -0.01 |
| $F_{554}$ | -0.0448   | $F_{3333}$ | 299.39   | $F_{6631}$ | 0.27   | $F_{7766}$ | 0.04   | $F_{9975}$ | 0.16  |
| $F_{651}$ | 0.2463    | $F_{4111}$ | -3.18    | $F_{6632}$ | -1.49  | $F_{7775}$ | 0.18   | $F_{9976}$ | 0.07  |
| $F_{652}$ | -2.1510   | $F_{4211}$ | 4.07     | $F_{6633}$ | 299.62 | $F_{7776}$ | 0.10   | $F_{9977}$ | 0.58  |
| $F_{653}$ | -0.6691   | $F_{4221}$ | -4.80    | $F_{6641}$ | -0.28  | $F_{7777}$ | 1.67   | $F_{9988}$ | 1.75  |
| $F_{654}$ | 0.0869    | $F_{4222}$ | 4.80     | $F_{6642}$ | 0.22   | $F_{8811}$ | 0.03   | $F_{9999}$ | 1.94  |

azide anions (Kelly et al. 2018). The proton-bound complexes shuttle nearly all of the charge and nearly none of the mass back and forth creating a huge induced dipole shift in the hydrogen atom's antisymmetric stretch. Here in NCNCN<sup>-</sup> the effect is slightly different in that the bond order is decreasing in one direction of the individual carbon atom's movement and increasing in the other, and there are two such motions happening conversely on opposite sides of the molecule. Consequently, a significant amount of electronic charge is moving in one direction across the entire molecule in much the same way but to a lesser extent than what happens in a plasmon. Additionally, this region of the infrared is relatively quiet in most astronomical spectra with few molecules exhibiting much motion due to the gulf in mass between hydrogen and any astrophysically meaningful heavier atoms. Granted, there are some lines and even a few bright ones. Hence, this molecule could serve to be a possible carrier in this region.

Additionally, the  $\nu_1$  fundamental at 2190.7 cm<sup>-1</sup> or 4.565  $\mu$ m is also notable but not nearly as bright. The same bond order increases and decreases are still happening due again to the motion of the internal carbon atoms, but now they are in concert only pushing the charge toward the central N<sub>1</sub> atom. Regardless, these two vibrational frequencies are probably convolved due to their close frequencies and wavelengths with  $\nu_2$  dominating to a significant extent. Even so, they both should be clear markers for observations with NIRSpect on the upcoming *James Webb Space Telescope* (JWST).

The  $\nu_3$  fundamental at 1302.3 cm<sup>-1</sup> or 7.679  $\mu$ m is predicted to be of the same intensity magnitude as the  $\nu_1$  but much more reddened. With an antisymmetric stretch of the terminal nitrogen atoms, the amount of charge movement is not as great as  $\nu_2$  since each nitrogen atom is only bonded to one carbon atom. Even so, this fundamental will likely not be observable astronomically as it sits squarely in a region almost certainly dominated by



**Table 3**The CcCR and F12-TZ QFF VPT2 Harmonic and Anharmonic Vibrational Frequencies in  $\text{cm}^{-1}$  with Intensities in  $\text{km mol}^{-1}$  <sup>a</sup>

|                  | Description         | CcCR   | F12-TZ | Intensity |
|------------------|---------------------|--------|--------|-----------|
| $\omega_1 (a_1)$ | C symm. stretch     | 2232.7 | 2224.5 | (97)      |
| $\omega_2 (b_2)$ | C antisymm. stretch | 2205.4 | 2197.7 | (1124)    |
| $\omega_3 (b_2)$ | N antisymm. stretch | 1322.9 | 1314.7 | (129)     |
| $\omega_4 (a_1)$ | N symm. stretch     | 920.8  | 918.3  | (17)      |
| $\omega_5 (b_2)$ | symm. N—C—N bend    | 670.8  | 668.2  | (3)       |
| $\omega_6 (a_2)$ | antisymm. OPB       | 553.5  | 549.4  |           |
| $\omega_7 (b_2)$ | antisymm. N—C—N     | 539.1  | 534.2  | (5)       |
| $\omega_8 (b_1)$ | symm. OPB           | 514.2  | 509.9  | (17)      |
| $\omega_9 (a_1)$ | C—N—C bend          | 165.9  | 165.8  | (5)       |
| $\nu_1 (a_1)$    | C symm. stretch     | 2190.7 | 2185.5 |           |
| $\nu_2 (b_2)$    | C antisymm. stretch | 2130.9 | 2123.8 |           |
| $\nu_3 (b_2)$    | N antisymm. stretch | 1302.3 | 1293.7 |           |
| $\nu_4 (a_1)$    | N symm. stretch     | 901.3  | 894.1  |           |
| $\nu_5 (b_2)$    | symm. N—C—N bend    | 661.0  | 660.5  |           |
| $\nu_6 (a_2)$    | antisymm. OPB       | 549.0  | 544.9  |           |
| $\nu_7 (b_2)$    | antisymm. N—C—N     | 532.4  | 527.9  |           |
| $\nu_8 (b_1)$    | symm. OPB           | 510.3  | 505.4  |           |
| $\nu_9 (a_1)$    | C—N—C bend          | 162.6  | 164.0  |           |
| ZPVE             |                     | 4535.9 | 4515.9 |           |
| $2\nu_1$         |                     | 4369.1 | 4358.8 |           |
| $\nu_1 + \nu_2$  |                     | 4329.4 | 4320.0 |           |
| $2\nu_2$         |                     | 4312.1 | 4303.4 |           |
| $\nu_1 + \nu_3$  |                     | 3479.7 | 3465.8 |           |
| $\nu_2 + \nu_3$  |                     | 3450.0 | 3436.9 |           |
| $2\nu_3$         |                     | 2577.7 | 2560.5 |           |

**Note.**<sup>a</sup> Double-harmonic MP2/6-31+G(d) intensities.

polycyclic aromatic hydrocarbons (PAHs). Hence, this frequency could assist in laboratory analysis but likely not in astrophysical classification.

The rest of the fundamental vibrational frequencies are relatively dim and will be further clouded by the myriad of other infrared features from various other molecular systems such as PAHs or silicates much more active below  $1000 \text{ cm}^{-1}$ , or  $10 \mu\text{m}$ . However, the overtones and combination bands of the bright fundamentals could be observed in near-IR, especially with *JWST* and SOFIA (the Stratospheric Observatory for Infrared Astronomy). The best candidate is the  $2\nu_2$  at  $4312.1 \text{ cm}^{-1}$  or  $2.319 \mu\text{m}$  due to the large intensity of the fundamental. The two combination bands of  $\nu_2$  with the other bright fundamentals ( $\nu_1 + \nu_2$  and  $\nu_2 + \nu_3$ ) could also possibly be observed at  $4329.4 \text{ cm}^{-1}$  ( $2.304 \mu\text{m}$ ) and  $3450.0 \text{ cm}^{-1}$  ( $2.899 \mu\text{m}$ ), respectively. However, the  $\nu_1 + \nu_2$  would probably be conjoined with  $2\nu_2$  much more than even the  $\nu_1$  and  $\nu_2$  fundamentals would, making  $\nu_1 + \nu_2$  a shoulder on the taller  $2\nu_2$  peak at best. The  $\nu_2 + \nu_3$  overtone could also be observed but likely only in regions where this anion is highly abundant.

In a general sense for this molecule, none of the fundamentals are highly anharmonic as would be expected for a molecule with no hydrogen atoms present. The  $\nu_1$  fundamental has an anharmonicity on the order of  $40 \text{ cm}^{-1}$  which still requires some type of anharmonic computation in order to begin to match laboratory or interstellar observations. The  $\nu_2$  fundamental has an anharmonicity reduction of slightly less at around  $35 \text{ cm}^{-1}$ . Hence, static scaling factors on harmonic computations could not reproduce the likely reliability of the frequency values here.

Additionally, the CcCR and F12-TZ QFF results match very closely for the vibrational frequencies, especially in the anharmonic values. The largest difference is for  $\nu_3$  at  $8.6 \text{ cm}^{-1}$ , and most are less than  $5.0 \text{ cm}^{-1}$  in line with what has previously been shown for closed-shell molecules even anions (Agbaglo & Fortenberry 2019). Hence, the values produced here give no indication of any irregularities and should assist in further spectral characterization of this markedly stable anion.

**4. Conclusions**

Using a quantum chemical analysis, we have demonstrated that  $\text{C}_2\text{N}_3^-$  displays a notable  $\nu_2$  fundamental vibrational frequency at  $2130.9 \text{ cm}^{-1}$  ( $4.693 \mu\text{m}$ ) carried by an antisymmetric stretch of the carbon atoms, while their symmetric  $\nu_1$  stretch vibration occurs at  $2190.7 \text{ cm}^{-1}$  ( $4.565 \mu\text{m}$ ). The two terminal nitrogen atoms carry the antisymmetric stretch fundamental  $\nu_3$  at  $1302.3 \text{ cm}^{-1}$  ( $7.679 \mu\text{m}$ ), a region rich in PAHs. Near-IR combination and overtone bands are present below  $2.9 \mu\text{m}$  and could also be used for astrochemical observations, such as the  $2\nu_2$  at  $4312.1$  ( $2.319 \mu\text{m}$ ). The F12-TZ approach is once more shown to be as reliable as the CcCR protocol indicating that it will continue to be useful for future work in this area. Overall, these quantum chemical calculations should aid in the search and detection of this remarkably stable anion in astrochemically relevant environments such as in the atmospheres of carbon-rich stars or Saturn's moon Titan, particularly in the era of the upcoming *JWST*.

R.C.F. acknowledges support from NASA grant NNX17AH15G, NSF grant OIA-1757220, and start-up funds provided by the University of Mississippi. D.D. expresses gratitude toward the NASA SMD (NNH17ZDA001N-CDAP) for funding, as well as Dr. Partha Bera for fruitful discussions. E.S.O. acknowledges support from NASA grants NNH17ZDA001N-CDAP and NNH17ZDA001N-SSW.

**ORCID iDs**David Dubois  <https://orcid.org/0000-0003-2769-2089>Ryan C. Fortenberry  <https://orcid.org/0000-0003-4716-8225>**References**

- Adler, T. B., Knizia, G., & Werner, H.-J. 2007, *JChPh*, **127**, 221106
- Agbaglo, D., & Fortenberry, R. C. 2019, *IJQC*, **119**, e25899
- Agbaglo, D., Lee, T. J., Thackston, R., & Fortenberry, R. C. 2019, *ApJ*, **871**, 236
- Allen, W. D. (ed.) 2005, INTDER 2005 is a General Program, which Performs Vibrational Analysis and Higher-Order Non-Linear Transformations
- Beilstein, F., & Geuther, A. 1858, *Liebig. Annal.*, **108**, 88
- Bizzocchi, L., Lattanzi, V., Laas, J., et al. 2017, *A&A*, **602**, A34
- Brünken, S., Gupta, H., Gottlieb, C. A., McCarthy, M. C., & Thaddeus, P. 2007, *ApJL*, **664**, L43
- Carrasco, N., Schmitz-Afonso, I., Bonnet, J. Y., et al. 2009, *JPCA*, **113**, 11195
- Coates, A. J., Cray, F. J., Lewis, G. R., et al. 2007, *GeoRL*, **34**, L22103
- Dahl, K., Sando, G. M., Fox, D. M., Sutto, T. E., & Owrutsky, J. C. 2005, *JChPh*, **123**, 084504
- de Jong, W. A., Harrison, R. J., & Dixon, D. A. 2001, *JChPh*, **114**, 48
- Desai, R. T., Coates, A. J., Wellbrock, A., et al. 2017, *ApJL*, **844**, 18
- Douglas, M., & Kroll, N. 1974, *AnPhy*, **82**, 89
- Dubois, D., Carrasco, N., Bourgalais, J., et al. 2019, *ApJL*, **872**, 31
- Dunning, T. H. 1989, *JChPh*, **90**, 1007
- Finney, B., Fortenberry, R. C., Francisco, J. S., & Peterson, K. A. 2016, *JChPh*, **145**, 124311
- Fortenberry, R. C. 2017, *IJQC*, **117**, 81
- Fortenberry, R. C., Crawford, T. D., & Lee, T. J. 2013, *ApJ*, **762**, 121

- Fortenberry, R. C., Huang, X., Crawford, T. D., & Lee, T. J. 2014a, *JPCA*, **118**, 7034
- Fortenberry, R. C., Huang, X., Francisco, J. S., Crawford, T. D., & Lee, T. J. 2011, *JChPh*, **135**, 134301
- Fortenberry, R. C., Huang, X., Francisco, J. S., Crawford, T. D., & Lee, T. J. 2012, *JChPh*, **136**, 234309
- Fortenberry, R. C., Huang, X., Schwenke, D. W., & Lee, T. J. 2014b, *AcSpA*, **119**, 76
- Fortenberry, R. C., Lee, T. J., & Müller, H. S. P. 2015a, *MolAs*, **1**, 13
- Fortenberry, R. C., Novak, C. M., Layfield, J. P., Matito, E., & Lee, T. J. 2018a, *J. Chem. Theor. Comput.*, **14**, 2155
- Fortenberry, R. C., Novak, C. M., & Lee, T. J. 2018b, *JChPh*, **149**, 024303
- Fortenberry, R. C., Yu, Q., Mancini, J. S., et al. 2015b, *JChPh*, **143**, 071102
- Franklin, E. C. 1922, *JACHS*, **44**, 3486
- Frisch, M. J., Trucks, G. W., Schlegel, H. B., et al. 2009, *Gaussian 09 Revision D.01* (Wallingford, CT: Gaussian Inc.)
- Gaw, J. F., Willets, A., Green, W. H., & Handy, N. C. 1991, in *Advances in Molecular Vibrations and Collision Dynamics*, ed. J. M. Bowman & M. A. Ratner (Greenwich, CT: JAI Press, Inc.), **170**
- Hehre, W. J., Ditchfield, R., & Pople, J. A. 1972, *JChPh*, **56**, 2257
- Huang, X., Fortenberry, R. C., & Lee, T. J. 2013, *JChPh*, **139**, 084313
- Huang, X., & Lee, T. J. 2008, *JChPh*, **129**, 044312
- Huang, X., & Lee, T. J. 2009, *JChPh*, **131**, 104301
- Huang, X., Taylor, P. R., & Lee, T. J. 2011, *JPCA*, **115**, 5005
- Huber, K. P., Herzberg, G., Gallagher, J. W., & Johnson, R. D., III 2018, in *Constants of Diatomic Molecules*, ed. P. J. Linstrom & W. G. Mallard (Gaithersburg, MD: National Institute of Standards and Technology), **69**
- Jagoda-Cwiklik, B., Wang, X. B., Woo, H. K., et al. 2007, *JPCA*, **111**, 7719
- Kelly, J. T., Ellington, T. L., Sexton, T. M., et al. 2018, *JChPh*, **149**, 191101
- Kendall, R. A., Dunning, T. H., & Harrison, R. J. 1992, *JChPh*, **96**, 6796
- Kitchens, M. J. R., & Fortenberry, R. C. 2016, *CP*, **472**, 119
- Knizia, G., Adler, T. B., & Werner, H.-J. 2009, *JChPh*, **130**, 054104
- Kong, L., Bischoff, F. A., & Valeev, E. F. 2011, *ChRv*, **112**, 75
- Lavvas, P., Yelle, R. V., Koskinen, T., et al. 2013, *PNAS*, **110**, 2729
- Maltseva, E., Petignani, A., Candian, A., et al. 2015, *ApJ*, **814**, 23
- Martin, J. M. L., & Lee, T. J. 1996, *CPL*, **258**, 136
- Martin, J. M. L., & Taylor, P. R. 1994, *CPL*, **225**, 473
- McCarthy, M. C., Gottlieb, C. A., Gupta, H., & Thaddeus, P. 2006, *ApJ*, **652**, L141
- McDonald, D. C., II, Mauney, D. T., Leicht, D., et al. 2016, *JChPh*, **145**, 231101
- McGuire, B. A. 2018, *ApJS*, **239**, 17
- Millar, T. J., Walsh, C., & Field, T. A. 2017, *ChRv*, **117**, 1765
- Mills, I. M. 1972, in *Molecular Spectroscopy—Modern Research*, ed. K. N. Rao & C. W. Mathews (New York: Academic), **115**
- Møller, C., & Plesset, M. S. 1934, *PhRv*, **46**, 618
- Nichols, C. M., Wang, Z. C., Yang, Z., Lineberger, W. C., & Bierbaum, V. M. 2016, *JPCA*, **120**, 992
- Papoušek, D., & Aliev, M. R. 1982, *Molecular Vibration-Rotation Spectra* (Amsterdam: Elsevier)
- Raghavachari, K., Trucks, G. W., Pople, J. A., & Head-Gordon, M. 1989, *CPL*, **157**, 479
- Remijan, A. J., Hollis, J. M., Lovas, F. J., et al. 2007, *ApJL*, **664**, L47
- Schimpl, A., Lemmon, R. M., & Calvin, M. 1965, *Sci*, **147**, 149
- Somogyi, Á., Smith, M. A., Vuitton, V., Thissen, R., & Komáromi, I. 2012, *IJMSp*, **316**, 157
- Steinman, G., & Cole, M. N. 1967, *PNAS*, **58**, 735
- Steinman, G., Kenyon, D. H., & Calvin, M. 1966, *BBA—General Subjects*, **124**, 339
- Stephan, C. J., & Fortenberry, R. C. 2017, *MNRAS*, **469**, 339
- Thackston, R., & Fortenberry, R. C. 2018, *JMaCh*, **56**, 103
- Thaddeus, P., Gottlieb, C. A., Gupta, H., et al. 2008, *ApJ*, **677**, 1132
- Watson, J. K. G. 1977, in *Vibrational Spectra and Structure*, ed. J. R. Durig (Amsterdam: Elsevier), **1**
- Werner, H.-J., Knowles, P. J., Knizia, G., et al. 2015, *MOLPRO*, v 2015.1, a Package of ab Initio Programs
- Werner, H.-J., Knowles, P. J., Knizia, G., Manby, F. R., & Schütz, M. 2012, *WIREs Comput. Mol. Sci.*, **2**, 242
- Yu, Q., Bowman, J. M., Fortenberry, R. C., et al. 2015, *JPCA*, **119**, 11623
- Zhao, D., Doney, K. D., & Linnartz, H. 2014, *ApJL*, **791**, L28